

## Evidence for Doorway States in $^{207}\text{Pb}$ , $^{208}\text{Pb}$ , and $^{57}\text{Fe}$ from Threshold Photoneutron Cross-Section Measurements\*

R. J. Baglan,† C. D. Bowman, and B. L. Berman

Lawrence Radiation Laboratory, University of California, Livermore, California 94550

(Received 9 November 1970)

The proposed doorway state in  $^{207}\text{Pb}$  seen by neutron total cross-section measurements on  $^{206}\text{Pb}$  also has been observed in the  $(\gamma, n)$  reaction. Both the envelope of the strength and the correlation between fine structure in the two channels support the doorway-state interpretation. The width for  $\gamma$ -ray decay of the doorway state to the ground state  $\Gamma_{\gamma_0}^D$  is found to be  $36.5 \pm 3.5$  eV. Other possible doorway states in the  $\gamma$ -ray channel in  $^{208}\text{Pb}$  at 500 keV,  $^{207}\text{Pb}$  at 125 keV, and  $^{57}\text{Fe}$  at 50 and 250 keV above threshold are discussed. An attempt is made to produce a correlation between neutron and  $\gamma$ -ray widths; no significant correlation was observed for these nuclei.

### I. INTRODUCTION

In 1963, Block and Feshbach<sup>1</sup> pointed out the possibility of the existence of "doorway" states. These states represent the first step, following the decay of a single-particle state, towards the formation of the compound nucleus; examples<sup>2</sup> are two-particle-one-hole (2p-1h) states or various collective states. If the coupling between the doorway state and the compound states is not too strong, the mean life of the doorway state will be intermediate between the long compound-nucleus lifetimes and the short lifetimes of single-particle states, and the doorway state might give rise to intermediate structure in the cross section. This structure will be characterized by a width which is large compared with compound-nucleus widths, but small compared with single-particle widths. These intermediate widths are estimated to be of the order of 100 keV.

The most common way to detect the presence of a doorway state is to observe structure of intermediate width in averaged cross-section data. However, this is not a definite determination. Structure of intermediate width might originate just from expected statistical fluctuations in level density and resonance widths. Also, before an intermediate structure can be interpreted to result from the presence of a doorway state, one must know that nearly all of the compound levels contributing to the structure have the same spin and parity  $J^\pi$ . Experimental data other than the average cross section for one channel are needed to determine definitely the presence of doorway states. Intermediate structure in more than one reaction channel leading to the same compound nucleus is obviously better; however, the best evidence is a correlation<sup>2,3</sup> between the widths for decay into two different exit channels for the fine-structure resonances of the doorway state.

The last method is applied here to the doorway state discovered<sup>4</sup> in  $^{207}\text{Pb}$  in neutron total cross-section measurements on  $^{206}\text{Pb}$ . In the measurements reported here, a similar envelope of ground-state  $\gamma$ -ray widths was found from threshold photoneutron cross-section measurements on  $^{207}\text{Pb}$ . The correlation between the neutron and  $\gamma$ -ray widths of the fine-structure resonances of the doorway is discussed, and from the correlation coefficient, the ground-state  $\gamma$ -ray width of the doorway state is determined. Possible additional doorway states at 125 keV above the  $(\gamma, n)$  threshold in  $^{207}\text{Pb}$ , 500 keV in  $^{208}\text{Pb}$ , and 50 and 250 keV in  $^{57}\text{Fe}$  are discussed. Also, an attempt is made to observe in  $^{57}\text{Fe}$  and  $^{53}\text{Cr}$  the channel-resonance effect of Lane and Lynn, which could be confused with doorway-state correlations.

### II. INTERMEDIATE STRUCTURE FROM EXPECTED STATISTICAL FLUCTUATIONS

Probably the best example of a doorway state detected by neutron-induced reactions was discovered in  $^{207}\text{Pb}$  by Farrell *et al.*<sup>4</sup> in high-resolution measurements of the neutron total cross section for  $^{206}\text{Pb}$ . In the energy range of their experiment, only elastic scattering and radiative-capture channels are open. They found a number of  $s$ -wave ( $J^\pi = \frac{1}{2}^+$ ) states in the energy region near 500 keV, which were analyzed by multilevel shape analysis<sup>5</sup> to obtain values for the neutron widths, in the excellent approximation  $\Gamma_n \approx \Gamma$ . The values of the reduced neutron widths  $\Gamma_n^0$  show an envelope, Fig. 1(a), whose width is  $\sim 250$  keV, whereas away from the energy position of this envelope there is little  $\frac{1}{2}^+$  neutron strength. This envelope was taken to represent a doorway state with a spin of  $\frac{1}{2}^+$ , and with fine structure representing more complex configurations, perhaps 3p-2h states. The measured neutron width of the doorway is consis-

tent with Shakin's<sup>6</sup> calculation of reduced neutron widths of (2p-1h) doorway states in <sup>207</sup>Pb.

Structure of intermediate width can result from expected random fluctuations in resonance widths and spacings.<sup>7</sup> In order to study this effect, a sample cross section was generated from resonance parameters which were chosen in a random fashion from appropriate distributions. The resonance widths  $\Gamma$  were chosen from a Porter-Thomas<sup>8</sup> distribution:  $P(X) = (1/\sqrt{2\pi}) X^{-1/2} e^{-X/2}$  where  $X = \Gamma/\langle\Gamma\rangle$ , and the level spacing  $S$  from a Wigner<sup>9</sup> distribution:  $P(Y) = (\pi Y/2) e^{-\pi Y^2/4}$ , where  $Y = S/\langle D\rangle$  and  $\langle D\rangle$  is the average level spacing. A typical portion of this generated function is shown in Fig. 2. The position of each vertical line in the lower plot indicates the position of a resonance, and the height of the line represents the reaction width. The curve in the upper plot, which is proportional to the average cross section, was calculated using a square smoothing function of breadth  $8\langle D\rangle$ . The dashed line in this plot is the mean cross section.

The average cross section was examined for the number of intermediate structures which one might associate with doorway states. The criteria for such a structure were arbitrarily selected to

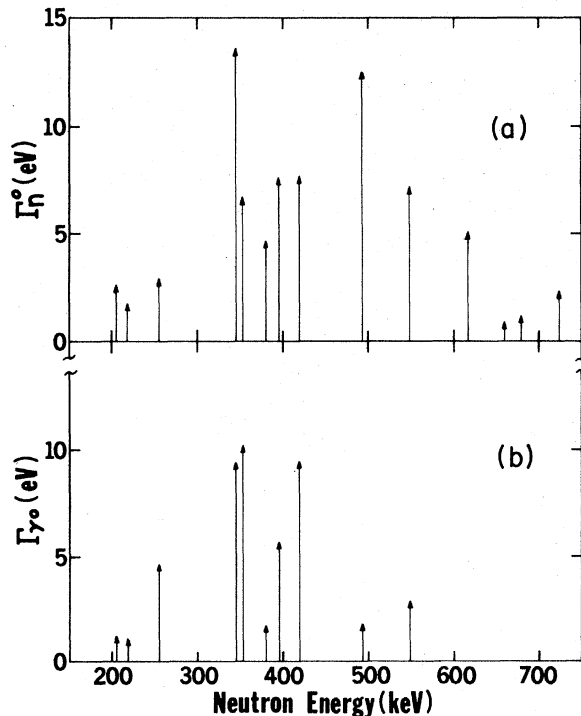


FIG. 1. Reduced neutron widths (a) and ground-state  $\gamma$ -ray widths (b) for  $\frac{1}{2}^+$  resonances in the <sup>207</sup>Pb compound nucleus. The positions of the arrows represent the resonance energies; their heights, the values of the widths. The resonance energies are the laboratory neutron energies measured in the  $(\gamma, n)$  experiment.

be: (1) that its height be at least 1.5 times the mean cross section; and (2) that the structure be made up of at least 10 resonances. Over each energy range corresponding to 1000 resonances, an average of 15 such structures were observed. Therefore, on the average, there is one statistically-generated "doorway state" per  $1000/15 = 67$  resonances. Or if, for example, the average level spacing is 10 keV, there is one statistical structure per 670 keV. Thus, there appears to be a rather frequent occurrence of intermediate structure from statistical fluctuations, and care must be taken in associating such structure with doorway states.

The <sup>207</sup>Pb doorway state discussed above consists of 14 resonances. The random analysis generated intermediate structures consisting of at least 14 resonances at the rate of one structure per 100 resonances. Since the average level spacing of  $\frac{1}{2}^+$  states in <sup>207</sup>Pb is 40 keV, there should be one such statistical structure per 4000 keV. A fairly strong case therefore can be made for the existence of a doorway state with the neutron data alone. If so, it would be of great interest if it appeared as a common doorway in another channel as well.

### III. <sup>207</sup>Pb DOORWAY STATE SEEN THROUGH <sup>207</sup>Pb( $\gamma, n$ )

The purpose of this work was to attempt to observe the doorway state through a measurement of the <sup>207</sup>Pb( $\gamma, n$ ) cross section, and then to deter-

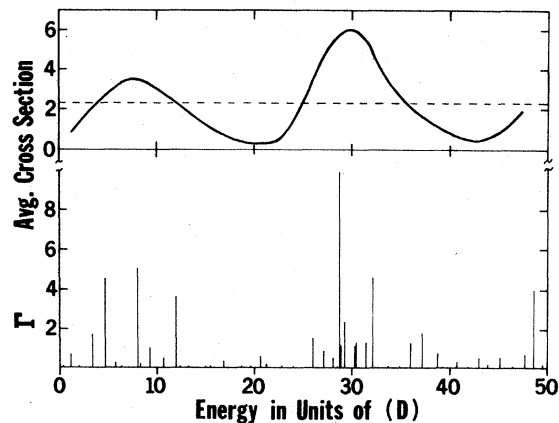


FIG. 2. A typical set of resonance widths and positions (lower plot) generated by a random choice of widths from a Porter-Thomas distribution and level spacings from a Wigner distribution. The energy scale is in units of the average level spacing  $\langle D\rangle$ . The solid curve (upper plot) is proportional to the average cross section generated from these parameters. The dashed line (upper plot) is the mean cross section. The ordinates have arbitrary units.

mine the ground-state  $\gamma$ -ray width of this state by measuring the correlation between the neutron and  $\gamma$ -ray widths of the fine-structure resonances of the doorway. The  $^{207}\text{Pb}(\gamma, n)$  cross section was measured using the threshold photoneutron technique.<sup>10-12</sup> In this experiment, bremsstrahlung from a pulsed, nearly monoenergetic electron beam is directed at a sample, and the neutrons ejected in the  $(\gamma, n)$  reaction are detected and their energy measured by the neutron time-of-flight technique. A proton-recoil neutron detector<sup>13</sup> was used, which provided fast and efficient detection of neutrons with energy greater than 100 keV. The over-all timing uncertainty in this experiment was about 0.7 nsec/m.

The results for  $^{207}\text{Pb}(\gamma, n)$ , from 200 to 700 keV, are shown in Fig. 3, where the differential cross section in mb/sr is plotted against the energy of the neutron emitted at  $135^\circ$  (on the lower scale) and the excitation energy (on the upper scale). The experimental resolution varies from 1.5 keV at low energies to 9.0 keV at high energies, while the uncertainty in the neutron energy scale is judged to be 1 to 2 keV. The measurements were made on a 143-g sample whose isotopic composition was 92.36%  $^{207}\text{Pb}$ , 5.48%  $^{208}\text{Pb}$ , and 2.16%  $^{208}\text{Pb}$ . To achieve the statistical accuracy of the data in Fig. 3, it was necessary to carry out the experiment with a bremsstrahlung end-point energy of 9.8 MeV (3.1 MeV above the photoneutron threshold). This introduced contamination into

the experiment from two sources. The isotopic contamination from  $^{208}\text{Pb}$  (photoneutron threshold 7.38 MeV) introduced peaks at 257 and 318 keV. These peaks can be located easily, and their influence taken into account by reference to other data<sup>14</sup> taken at this laboratory with an isotopically pure  $^{208}\text{Pb}$  sample. The other source of contamination is neutron emission from  $^{207}\text{Pb}$  to states other than the ground state of  $^{206}\text{Pb}$ . However, a measurement carried out with an end-point energy  $E_e = 7.35$  MeV, for which only ground-state neutron emission is possible, revealed essentially all the prominent features of the cross section seen with  $E_e = 9.8$  MeV, except for peaks at 244 and 533 keV.

Below 600 keV, the locations of 10  $\frac{1}{2}^+$  resonances could be assigned from neutron total cross-section measurements<sup>4</sup> on  $^{206}\text{Pb}$ . These resonances are indicated by the unlabeled arrows above the data in Fig. 3. For eight of the ten resonances, the position of the peak agrees within 1 keV with the position determined by the neutron experiment. [Recoil effects which result in lower neutron energies in the  $(\gamma, n)$  experiment have been taken into account.] For the resonance at 374 keV, the positions differ by 4 keV and for the 391-keV resonance they differ by 2 keV. Since the uncertainties in the determination of the resonance energies are about  $\pm 1$  keV in both this work and the neutron experiment, it appears that, except in the case of the 374-keV peak, the resonance energies agree very well. The  $\frac{1}{2}^+$  resonance near 374 keV

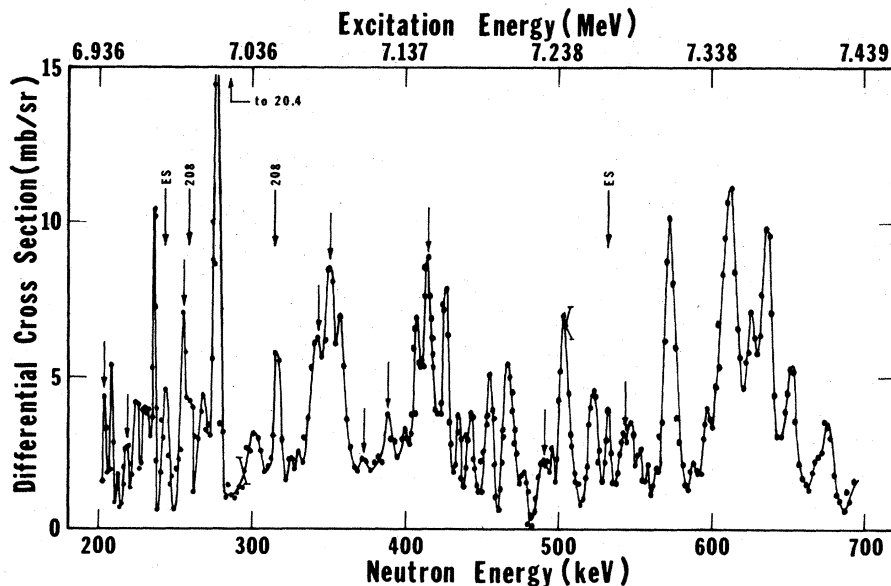


FIG. 3. The  $135^\circ$  differential  $^{207}\text{Pb}(\gamma, n)$  cross section as a function of the energy of the emitted neutron (on the lower scale) and the excitation energy (on the upper scale). The labeled arrows indicate peaks which correspond to transitions to excited states (ES) of  $^{206}\text{Pb}$  and peaks caused by the  $^{208}\text{Pb}$  contaminant in the sample. The 10 unlabeled arrows indicate peaks which correspond to  $\frac{1}{2}^+$  states.

might not have been seen in this work. The absence of this peak will not change any conclusions in this paper. The four  $\frac{1}{2}^+$  states which were seen in the neutron experiment above 600 keV are not included in the present analysis, since our resolution at these energies was not sufficient to resolve them from adjacent states. For example, a  $\frac{1}{2}^+$  resonance was seen in the neutron work at a position which corresponds to the strong peak at 613 keV in the  $^{207}\text{Pb}(\gamma, n)$  spectrum, Fig. 3. This peak is nearly resolved in the  $(\gamma, n)$  spectrum with a total width of 13 keV. However, its total width as measured in the neutron experiment is only 4 keV. Therefore, the 613-keV peak includes resonances other than the  $\frac{1}{2}^+$  state, and consequently information concerning the  $\frac{1}{2}^+$  peak alone cannot be obtained.

The area under a peak in the  $(\gamma, n)$  spectrum is given, with the usual notation, by  $2\pi^2\kappa^2 g_\gamma \Gamma_\gamma \Gamma_n / \Gamma$ . Using the excellent approximation,  $\Gamma_n / \Gamma = 1$ , the area is proportional to  $g_\gamma \Gamma_\gamma$ , independent of the neutron width and the resolution. The details of the analysis are given in another paper<sup>14</sup> which summarizes all the recent Livermore threshold photo-neutron data. In the determination of these areas for the  $\frac{1}{2}^+$  peaks, the effect of the other resonances must be taken into account. Most of the other peaks in the spectrum probably are  $\frac{3}{2}^+$  resonances which also are excited by  $E1$  photons from the ground state of  $^{207}\text{Pb}$ . Because of the  $2J+1$  rule for level densities, twice as many  $\frac{3}{2}^+$  as  $\frac{1}{2}^+$  resonances are expected, consistent with the observed spectrum. The  $\frac{3}{2}^+$  resonances decay by  $d$ -wave neutrons, but since  $\Gamma_n \gg \Gamma_\gamma$  even for these states, they will appear just as strongly in the  $(\gamma, n)$  spectrum as the  $\frac{1}{2}^+$  states (area  $\propto g_\gamma \Gamma_\gamma$ ). The  $\frac{3}{2}^+$  resonances have total widths much narrower than the measured widths shown in Fig. 3 (determined by the resolution function). Therefore, the level-level interference is much smaller than would at first appear and has been neglected. The high level density results in some overlapping of resonances. This limits the accuracy to which values for  $\Gamma_\gamma$  can be determined to an estimated  $\pm 25\%$ .

The ground-state  $\gamma$ -ray widths  $\Gamma_\gamma$  for the 10  $\frac{1}{2}^+$  states below 600 keV are listed, along with the corresponding reduced neutron widths  $\Gamma_n^0$ , in Table I. The values for  $\Gamma_\gamma$  are represented by vertical arrows in Fig. 1(b). The distribution of these values for  $\Gamma_\gamma$  shows an envelope very similar to that for  $\Gamma_n^0$ . The fact that envelopes of widths are seen in both reaction channels is very strong evidence for the existence of a common doorway. The frequency with which random fluctuations will give rise to envelopes near the same energies in two different reaction channels can be computed in a way which is analogous to the cal-

ulation of random coincidences between two independent counting rates. As mentioned earlier, the random analysis generates intermediate structures, similar to the one seen in  $^{207}\text{Pb}$ , at the rate of one per 4000 keV; the frequency with which two such structures will overlap within an energy interval of 200 keV is once per 40 MeV.

#### IV. DETERMINATION OF THE GROUND-STATE $\gamma$ -RAY WIDTH OF THE DOORWAY STATE FROM CORRELATION ANALYSIS

##### A. Correlation Expected Between Neutron and $\gamma$ -Ray Widths

The neutron and  $\gamma$ -ray widths for the fine-structure resonances of the doorway state should be correlated if indeed the same doorway state is seen in both channels. If such a correlation were found to exist, it would provide additional evidence for the existence of the doorway state and would allow the determination of the ground-state  $\gamma$ -ray width of the doorway state.

If one assumes that a doorway state is present, the wave function for the  $i$ th  $\frac{1}{2}^+$  level of the fine structure can be written as:

$$\psi_{Ti} = a_i \psi_D + \psi_{oi}, \quad (1)$$

where  $\psi_D$  is the doorway-state wave function and  $\psi_{oi}$  represents all other contributions to the total wave function. The reduced neutron widths and the ground-state  $\gamma$ -ray widths can be expressed as

$$\begin{aligned} \Gamma_{ni}^0 &= |\langle \psi_{206} | H_n | \psi_{Ti} \rangle|^2, \\ \Gamma_{\gamma oi} &= |\langle \psi_{207} | H_\gamma | \psi_{Ti} \rangle|^2, \end{aligned} \quad (2)$$

where  $\psi_{206}$  and  $\psi_{207}$  are the ground-state wave functions of  $^{206}\text{Pb}$  and  $^{207}\text{Pb}$ , respectively. By substituting Eq. (1) into Eqs. (2) one obtains:

TABLE I. Reduced neutron widths and ground-state  $\gamma$ -ray widths for the 10  $\frac{1}{2}^+$  resonances considered in this work. The indicated resonance energies are the laboratory neutron energies measured in this experiment.

Energy (keV)	$\Gamma_n^0$ (eV) <sup>a</sup>	$\Gamma_\gamma$ (eV)
205	2.64	1.27
217	1.82	1.13
253	2.97	4.74
342	13.60	9.42
350	6.73	10.26
374	4.70	1.75
391	7.64	5.76
416	7.72	9.48
488	12.53	1.88
543	7.29	2.90

<sup>a</sup>See Ref. 4.

$$\Gamma_{ni}^0 = a_i^2 \Gamma_n^{0D} + \gamma_{ni} \pm 2(a_i^2 \Gamma_n^{0D})^{1/2} (\gamma_{ni})^{1/2}, \quad (3a)$$

$$\Gamma_{\gamma 0i} = a_i^2 \Gamma_{\gamma 0}^D + \gamma_{\gamma i} \pm 2(a_i^2 \Gamma_{\gamma 0}^D)^{1/2} (\gamma_{\gamma i})^{1/2}, \quad (3b)$$

where

$$\Gamma_n^{0D} = |\langle \psi_{206} | H_n | \psi_D \rangle|^2, \quad (4a)$$

$$\Gamma_{\gamma 0}^D = |\langle \psi_{207} | H_\gamma | \psi_D \rangle|^2, \quad (4b)$$

$$\gamma_{ni} = |\langle \psi_{206} | H_n | \psi_{0i} \rangle|^2, \quad (4c)$$

and

$$\gamma_{\gamma i} = |\langle \psi_{207} | H_\gamma | \psi_{0i} \rangle|^2. \quad (4d)$$

Equations (3a) and (3b) show that the neutron and  $\gamma$ -ray widths for individual resonances should be correlated. This is because both  $\Gamma_{ni}^0$  and  $\Gamma_{\gamma 0i}$  depend on the value of the coefficient  $a_i^2$ . If  $a_i^2$  is large for a particular resonance, then that resonance will have both large neutron and  $\gamma$ -ray widths. The degree of correlation will depend upon the relative size of the correlated terms ( $a_i^2 \Gamma_n^{0D}$  and  $a_i^2 \Gamma_{\gamma 0}^D$ ) with respect to the random terms ( $\gamma_{ni}$  and  $\gamma_{\gamma i}$ ); or, conversely, a measure of the degree of correlation can be used to determine the relative size of the correlated terms with respect to the random term. In this way  $\Gamma_{\gamma 0}^D$  can be obtained. (If either the  $a_i^2 \Gamma_n^{0D}$  terms are smaller than the  $\gamma_{ni}$  terms, or if the  $a_i^2 \Gamma_{\gamma 0}^D$  terms are smaller than the  $\gamma_{\gamma i}$  terms, then an envelope of widths will appear in only one channel and no correlation will exist. However, a doorway would exist in that channel even though the correlation analysis could not detect it.)

There are two questions to be answered concerning the possible correlation between the neutron and  $\gamma$ -ray widths: first, does a correlation exist, and second, what is the degree of correlation? Two different correlation coefficients will be computed in order to answer these questions. The *rank* correlation coefficient  $\rho$  tests the existence of correlation while the *product-moment* correlation coefficient  $r$  measures the degree of correlation but cannot be interpreted as exactly as  $\rho$  with respect to the existence of a correlation.

#### B. Existence of a Correlation

The great value of the rank correlation coefficient<sup>15</sup> is its use as a test of the existence of correlation, a test capable of exact interpretation in terms of probability without any assumption of normal or other special distributions for the sets under study. The rank correlation coefficient ignores the exact values of the individual members of the sets and thus does not measure the degree of correlation. This correlation coefficient is determined by first assigning to each member of the set a number corresponding to its ranking in size.

The largest member of the set is assigned the number 1, the next 2, etc. Then

$$\sum d^2 = \sum_{i=1}^N d_i^2 \quad (5)$$

is computed, where  $d_i$  is the rank difference between the  $i$ th pair of numbers. For example, in Table I the neutron width for the first resonance is the ninth largest neutron width and is assigned the number 9. Also, the  $\gamma$ -ray width for the first resonance is the ninth largest and also is assigned the number 9. The rank difference between the first pair is  $d_1 = (9 - 9) = 0$  and  $d_1^2 = 0$ . For the 10 pairs of widths,  $\sum d^2 = 66$ . The rank correlation coefficient is defined as  $\rho = 1 - 6 \sum d^2 / (N^3 - N)$ , where  $N$  is the number of values in each set. For the data of Table I,  $\rho = 0.60$ . Olds<sup>16</sup> gives tables for testing the significance of  $\rho$  or  $\sum d^2$ . For  $N = 10$ , the probability that  $\sum d^2 \leq 66$  is 0.036. Therefore, random effects alone are expected to result in a  $\sum d^2$  as low as 66 only 3.6% of the time, implying a probability of  $1 - 0.036 = 0.964$  that some correlation exists. This correlation is further evidence for the presence of a doorway state.

#### C. Degree of Correlation

The product-moment correlation coefficient for the neutron and  $\gamma$ -ray widths is given by

$$r = \frac{N \sum \Gamma_{\gamma 0i} \Gamma_{ni}^0 - \sum \Gamma_{\gamma 0i} \sum \Gamma_{ni}^0}{\left\{ [N \sum \Gamma_{\gamma 0i}^2 - (\sum \Gamma_{\gamma 0i})^2] [N \sum \Gamma_{ni}^0{}^2 - (\sum \Gamma_{ni}^0)^2] \right\}^{1/2}}, \quad (6)$$

where the summations are from  $i = 1$  to  $N$ . A value of 1 implies perfect correlation; 0, no correlation; and -1, perfect anticorrelation. Using the data of Table I,  $r = +0.44$ . The fact that this number is not close to 1 does not indicate a lack of correlation. It only indicates a correlation which is less than perfect, as expected, because of the random terms in Eqs. (3a) and (3b).

Before  $r$  is used to determine the ground-state  $\gamma$ -ray width of the doorway state  $\Gamma_{\gamma 0}^D$ , error limits will be calculated for  $r$ . These error limits will allow the determination of uncertainties in  $\Gamma_{\gamma 0}^D$ . The uncertainties in  $r$  arise from three sources: (1) random errors in the determination of the values for  $\Gamma_n^0$  and  $\Gamma_{\gamma 0}$ ; (2) systematic errors in the values for  $\Gamma_{\gamma 0}$  owing to the uncertainty in the background level under the resonances in Fig. 3; and (3) the possibility that the 374-keV resonance was not seen in this experiment and thus has  $\Gamma_{\gamma 0} = 0$ .

The effect of random errors in the values for  $\Gamma_n^0$  and  $\Gamma_{\gamma 0}$  was determined in the following way. The uncertainty for  $\Gamma_{\gamma 0}$  was taken to be  $\pm 20\%$  and for  $\Gamma_n^0$  to be  $\pm 10\%$ . A computer code then was used to vary randomly the measured neutron widths

within the limits of  $\pm 10\%$  and the measured  $\gamma$ -ray widths within  $\pm 20\%$ . A correlation coefficient was computed from these new widths. The distribution of many such correlation coefficients formed a bell-shaped curve with a mean value of 0.44 and with  $r$  values at half-maximum of 0.35 and 0.51. Therefore, the 10-to-20% uncertainties in the reaction widths result in an uncertainty of about  $\pm 18\%$  in  $r$ .

The variations in  $r$  arising from an uncertainty of  $\pm 0.5$  mb/sr in the background were determined first by decreasing the background by 0.5 mb/sr and computing  $r$  based on the new values for  $\Gamma_{\gamma 0}$ , and then by increasing the background and computing a corresponding  $r$ . The correlation coefficients computed in this way were, respectively, 0.46 and 0.43 implying an uncertainty of about  $\pm 3\%$  in  $r$ .

As mentioned earlier, the 373-keV resonance might not have been seen in the  $^{207}\text{Pb}(\gamma, n)$  measurement and thus might have  $\Gamma_{\gamma 0} = 0$ . If this value is used (instead of the measured 1.75 eV) in the determination of  $r$ , the new correlation coefficient

is  $r = 0.45$ . The combination of the three sources of uncertainty give limits of about  $\pm 20\%$  on the correlation coefficient, or  $0.35 \leq r \leq 0.53$ .

#### D. Determination of $\Gamma_{\gamma 0}^D$

The value of  $r$  now can be used to determine the ground-state  $\gamma$ -ray width of the doorway state  $\Gamma_{\gamma 0}^D$ . The total ground-state  $\gamma$ -ray width in the  $10^{\frac{1}{2}+}$  resonances is measured to be 48.6 eV. Referring to Eq. (3b), one sees that the  $a_i^2 \Gamma_{\gamma 0}^D$  terms and the  $\gamma_{\gamma i}$  terms will add to  $\sim 48.6$  eV since the cross terms, being random in sign, will tend to cancel out. The larger are the  $a_i^2 \Gamma_{\gamma 0}^D$  terms, compared with the  $\gamma_{\gamma i}$  terms, the larger will be the correlation coefficient; or if  $r$  is known, the relative size of the  $a_i^2 \Gamma_{\gamma 0}^D$  terms with respect to the  $\gamma_{\gamma i}$  terms can be determined. This was done in the following way. First, it is assumed that the last two terms in Eq. (3a) can be neglected. This assumption is based on the neutron total cross-section measurement<sup>4</sup> of  $^{208}\text{Pb}$ , in which very little neutron strength is seen outside of the energy region of the doorway state, indicating that nearly all of the neutron strength in this region comes from the doorway-state part of the wave function. Next, values for the  $a_i^2$  are computed using the measured neutron widths in Eq. (3a) where  $\sum_i a_i^2 = 1$ . Then a value for  $\Gamma_{\gamma 0}^D$  is chosen and the average value of  $r$  corresponding to this  $\Gamma_{\gamma 0}^D$  is calculated. This is done first by generating 10 random values for  $\gamma_{\gamma i}$  from a Porter-Thomas distribution, subject to the constraint that the average of these widths is  $\langle \gamma_{\gamma i} \rangle = (\frac{1}{10})(48.6 - \Gamma_{\gamma 0}^D)$ . 10 values of  $\Gamma_{\gamma 0 i}$  then are computed from Eq. (3b) using the random values of  $\gamma_{\gamma i}$ , the chosen  $\Gamma_{\gamma 0}^D$ , the set of coefficients  $a_i$ , and random signs for the third term. Finally,  $r$  is calculated between these values for  $\Gamma_{\gamma 0 i}$  and those for  $\Gamma_{\gamma 0}^D$ . The average of many such values of  $r$ , calculated with the same  $\Gamma_{\gamma 0}^D$  but different sets of values for  $\gamma_{\gamma i}$ , will be positive since we are assuming that a doorway state is present, i.e.,  $\Gamma_{\gamma 0}^D > 0$ . This average  $r$  will be a function of the chosen  $\Gamma_{\gamma 0}^D$ . Figure 4 shows the results of this analysis, where  $\Gamma_{\gamma 0}^D$  is plotted against  $r$ . The experimental correlation coefficient of 0.44 is found to be associated with  $\Gamma_{\gamma 0}^D = 36.5$  eV. The limits of  $\pm 20\%$  on  $r$  set the following limits on  $\Gamma_{\gamma 0}^D$ :  $33 \leq \Gamma_{\gamma 0}^D \leq 40$  eV.

In summary, the  $10^{\frac{1}{2}+}$  compound-nucleus resonances seen in the  $^{208}\text{Pb}$  neutron-scattering experiment below 600 keV were seen in this work through a different reaction channel,  $^{207}\text{Pb}(\gamma, n)$ .  $\Gamma_{\gamma 0}^D = 36.5$  eV. The total  $\gamma$ -ray width of the  $10^{\frac{1}{2}+}$  resonances is 48.6 eV, indicating that most of the  $\gamma$ -ray strength (75%) is derived from the doorway-state portion of the wave function. The value, 36.5 eV, is about an order of magnitude smaller

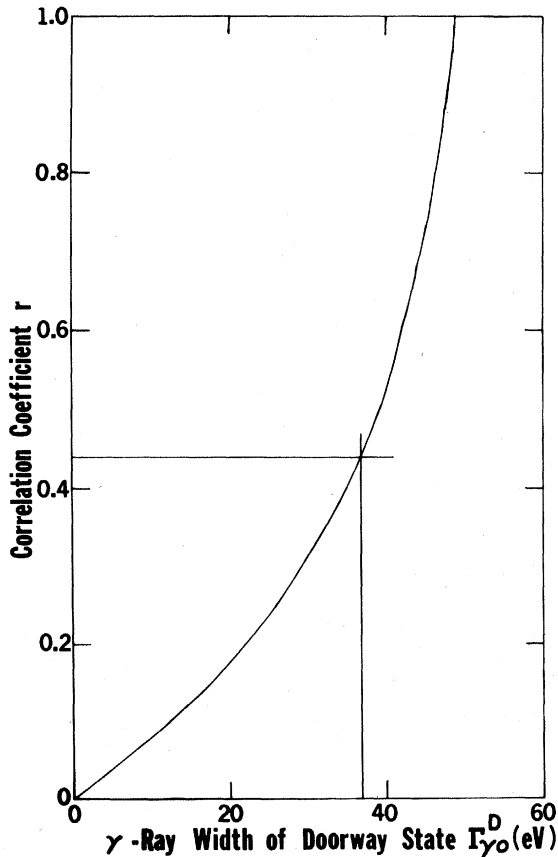


FIG. 4.  $\Gamma_{\gamma 0}^D$  versus the product-moment correlation coefficient  $r$  for 10 resonances having a total  $\gamma$ -ray width of 48.6 eV.

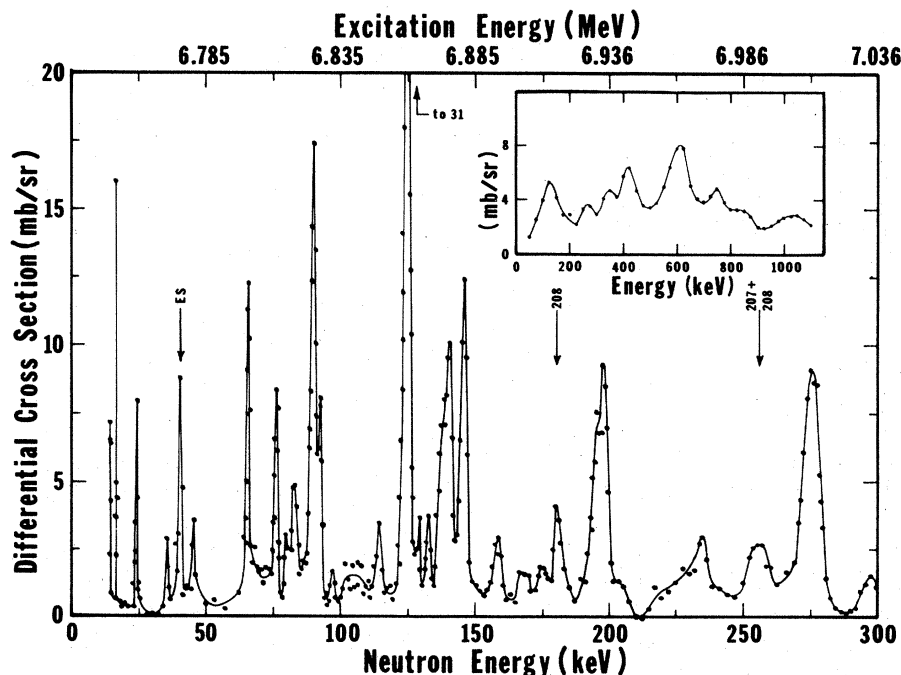


FIG. 5. The  $135^\circ$  differential  $^{207}\text{Pb}(\gamma, n)$  cross section. The arrows indicate contaminating peaks caused by the isotopic contaminant  $^{208}\text{Pb}$ , and transitions to excited states (ES) of  $^{206}\text{Pb}$ . The inset shows the  $(\gamma, n)$  cross section averaged with a 40-keV square smoothing function.

than the single-particle width calculated for an electric dipole transition in  $^{207}\text{Pb}$ . Most of the  $\gamma$ -ray strength of the single-particle state apparently has been transferred into the giant dipole resonance in accordance with the model of Brown.<sup>17</sup> The residual strength which is measured here perhaps is typical of the many single-particle states possible in  $^{207}\text{Pb}$ .

It should be noted that there is another mechanism which can give rise to a correlation between neutron and  $\gamma$ -ray widths. This is the channel-resonance effect<sup>18</sup> of Lane and Lynn, as will be discussed in Sec. VII of this paper. However, since the envelopes of neutron and  $\gamma$ -ray widths coincide for  $^{207}\text{Pb}$  the evidence is very strong that the correlation results from the presence of a doorway state and not from the channel-resonance effect.

#### V. OTHER DOORWAY STATES

Additional threshold photoneutron cross sections were measured and examined for the presence of doorway states. These measurements are discussed in Ref. 14 and include:  $^{206}, ^{208}\text{Pb}$ ,  $^{207}\text{Pb}$  (below 200 keV),  $^{56}, ^{57}\text{Fe}$ ,  $^{52}, ^{53}\text{Cr}$ , and  $^{24}, ^{25}, ^{26}\text{Mg}$ . Possible evidence for doorway states in the form of intermediate structures and/or envelopes of  $\gamma$ -ray widths was observed in  $^{207}\text{Pb}$  near 125 keV,  $^{208}\text{Pb}$  near 500 keV, and  $^{57}\text{Fe}$  near 50 and 250 keV above

the photoneutron threshold. These are discussed in detail below.

#### A. $^{207}\text{Pb}$ near 125 keV

Figure 5 shows the  $^{207}\text{Pb}(\gamma, n)$  cross section below 200 keV. The multiplicity neutron detector<sup>19</sup> was used for this measurement and the bremsstrahlung end-point energy was 8.4 MeV. The 40-keV peak is associated with a neutron transition to an excited state of  $^{206}\text{Pb}$ . The isotopic contaminant  $^{208}\text{Pb}$  introduced a peak at 182 keV and contributed to the 257-keV peak. These peaks are

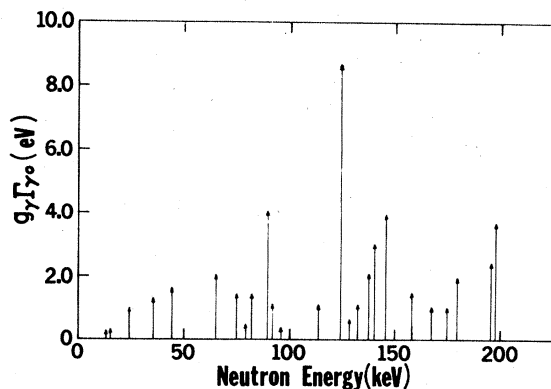


FIG. 6. Values for  $g_\gamma \Gamma_{\gamma_0}$  for the resonances in  $^{207}\text{Pb}(\gamma, n)$  below 200 keV.

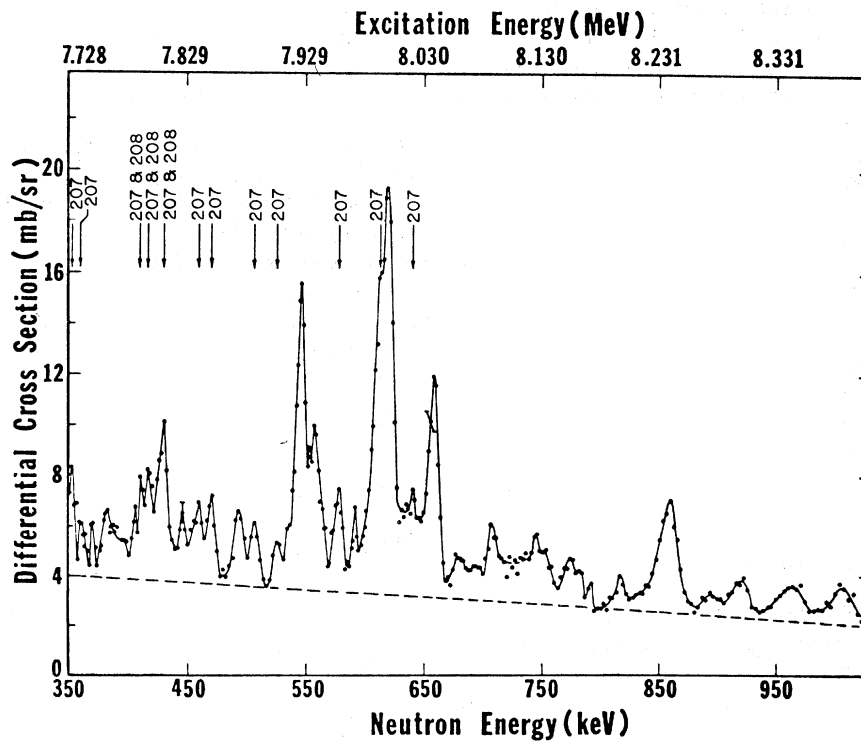
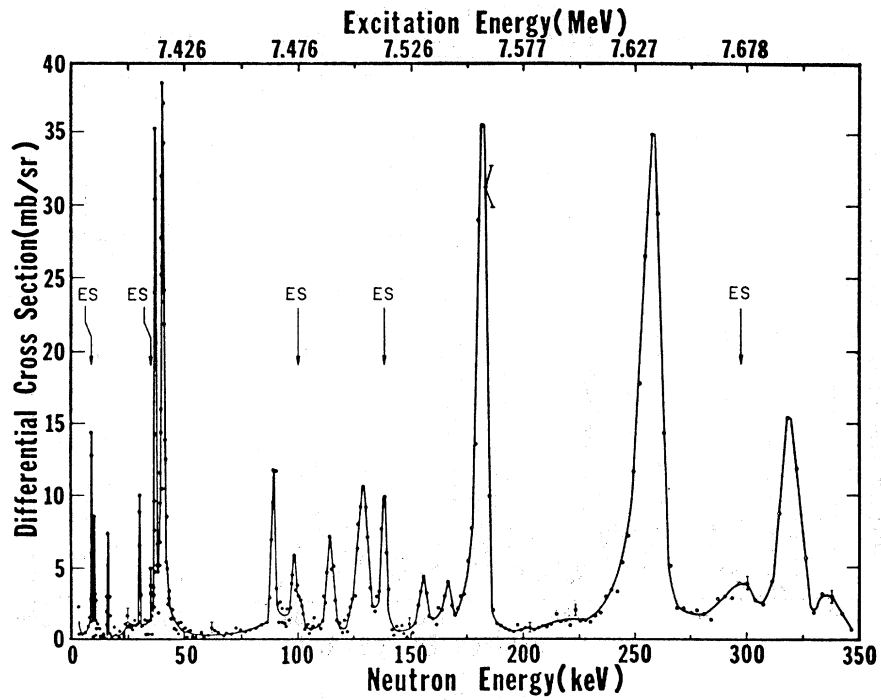


FIG. 7. The  $135^\circ$  differential  $^{208}\text{Pb}(\gamma, n)$  cross section. Arrows labeled ES denote resonances associated with transitions to excited states of  $^{207}\text{Pb}$ . Arrows in the lower plot denote peaks caused by the isotopic contaminant  $^{207}\text{Pb}$ . The dashed line in the lower plot represents the experimental background.



indicated by arrows in Fig. 5.

Very little  $s$ -wave ( $J^\pi = \frac{1}{2}^+$ ) strength was seen in the  $^{206}\text{Pb}$  neutron total cross section below 200 keV. This cross section is given in the work of Macklin, Pasma, and Gibbons<sup>20</sup> for  $10 < E_n < 80$  keV, in Ref. 4 for  $E_n > 135$  keV, and in the work of Bilpuch *et al.*<sup>21</sup> for  $50 < E_n < 200$  keV. Below 200 keV, only one peak, at 66 keV, is assigned a  $J^\pi = \frac{1}{2}^+$ . Therefore, most of the peaks in Fig. 5 probably are  $\frac{3}{2}^+$  resonances which are excited by  $E1$  photons from the ground state of  $^{207}\text{Pb}$  and which decay by  $d$ -wave neutrons. (Biggerstaff *et al.*<sup>22</sup> assign  $J^\pi$  of  $\frac{1}{2}^-$  or  $\frac{3}{2}^-$  to four of the peaks below 50 keV, based on the fact that they have  $l > 0$  and decay by photons to  $\frac{1}{2}^-$ ,  $\frac{3}{2}^-$ , and  $\frac{5}{2}^-$  states. However, the evidence is consistent with an assignment of  $\frac{3}{2}^+$ , where the  $\gamma$ -ray transitions then would go by  $E1$  photons.) The averaged  $(\gamma, n)$  cross section (inset, Fig. 5) contains a peak centered at 125 keV. This structure might represent a  $\frac{3}{2}^+$  doorway state. The ground-state  $\gamma$ -ray widths for the resonances below 200 keV were determined from area analysis and are represented by the arrows in Fig. 6. The values for  $\Gamma_{\gamma 0}$  form an envelope whose width is 120 keV. There are 25 resonances contributing to this envelope. This large number of resonances tends to rule out statistical fluctuations as the cause of the structure. The cross section generated by randomly-chosen parameters (Sec. III) shows intermediate structures containing 20 or more resonances occurring at the rate of 1 per 500 resonances; or for the density of states below 200 keV, 1 per 4 MeV. Therefore, the 125-keV structure probably is not statistical, but instead represents a  $\frac{3}{2}^+$  doorway state. Such a state is expected on the basis of the configuration discussed in Ref. 4 by simply recoupling the  $\frac{1}{2}^-$  neutron hole and the  $1^-$  particle-hole or collective state to give a  $\frac{3}{2}^+$  doorway in addition to the  $\frac{1}{2}^+$  doorway state. [It should be mentioned that the intermediate structure seen here could represent an  $M1$  doorway state with  $J^\pi = \frac{1}{2}^-$  or  $\frac{3}{2}^-$  (see Bowman *et al.*<sup>23</sup>).]

The ground-state  $\gamma$ -ray width of this doorway state cannot be determined as it was for the 500-keV doorway state since the  $d$ -wave neutron widths have not been measured. However, it can be estimated from the area under the peak in the average cross section (inset, Fig. 5). A background level of 2.6 mb/sr is drawn under the peak and subtracted from the area to account for the contribution to the  $\gamma$ -ray width from that part of the wave function not associated with the doorway state. The remaining area under the peak is 2.7 keVb, where the effect of the nonisotropic distribution of the  $d$ -wave neutrons has been accounted for. This area analysis gives  $\Gamma_{\gamma 0}^D = 16.3$  eV.

#### B. $^{208}\text{Pb}$ near 500 keV

The  $135^\circ$  differential  $^{208}\text{Pb}(\gamma, n)$  cross section is shown in Fig. 7. The low-energy data (upper plot) were taken with a sample enriched to 99.75% in  $^{208}\text{Pb}$ , using the multiplicity neutron detector. The high-energy data were taken with a natural lead sample, using the proton-recoil neutron detector. Both measurements were made with a bremsstrahlung end-point energy of 9.8 MeV. Additional measurements performed at lower energies identified peaks which correspond to neutron decay to excited states of  $^{207}\text{Pb}$  (designated by ES in Fig. 7). The isotopic contaminant  $^{207}\text{Pb}$  introduces many peaks in the high-energy data. The prominent peaks at 547, 620, 660, and 860 keV are resonances in  $^{208}\text{Pb}$  associated with ground-state transitions. No prominent peaks were observed between 860 and 1200 keV.

The spins of most of the prominent resonances in Fig. 7 were determined by comparing these data measured at  $135^\circ$ , with similar measurements carried out at  $90^\circ$ . The multiplicity detector measured the cross section at both angles over the energy range from 10 to 1000 keV, and the proton-recoil detector was used at both angles from 130 to 1200 keV. The ratio of the cross sections at the two angles was compared with theoretical values in order to determine values for  $J^\pi$ . (This analysis is discussed in detail in Ref. 23.) The results indicate a large number of  $1^+$  states. The seven resonances located at 30.2, 114, 182, 318, 620, 660, and 860 keV were assigned  $J^\pi = 1^+$ . The total  $\gamma$ -ray strength in these  $M1$  resonances, as determined from area analysis, is  $50.8_{-10}^{+14}$  eV.

This  $M1$  strength in  $^{208}\text{Pb}$  arises from spin-flip transitions from the  $i_{13/2}$  neutron shell and the  $h_{11/2}$  proton shell. These particle-hole states form the doorway state through which the compound-nucleus states observed here are reached. The total  $\gamma$ -ray strength for these states constitutes at least half and perhaps all of the total  $M1$  strength calculated for this nucleus.<sup>24</sup>

#### C. $^{57}\text{Fe}$ near 50 keV

Figures 8 and 9 show the  $^{57}\text{Fe}(\gamma, n)$  cross section. This was measured using the multiplicity detector with a bremsstrahlung end-point of 11.5 MeV. The sample was 51.5 g of  $\text{Fe}_2\text{O}_3$  enriched to 90.4% in  $^{57}\text{Fe}$ . Low-energy runs showed that the strong resonances are associated with ground-state neutron transitions,<sup>14</sup> but could not determine whether the weaker peaks decay to the ground or to some excited state of  $^{56}\text{Fe}$ . The arrows below the data indicate the positions of  $\frac{1}{2}^+$  states as determined by neutron total cross-section measurements<sup>5</sup> on  $^{56}\text{Fe}$ . The inset in Fig. 9

shows the  $^{57}\text{Fe}(\gamma, n)$  cross section averaged with a 40-keV square smoothing function. The dashed curve in the inset is the smoothed neutron total cross section<sup>25</sup> for  $^{56}\text{Fe}$  showing the broad structures at 400 and 800 keV which have been suggested as positions of doorway states. No strong correlation was found between this curve and the averaged  $(\gamma, n)$  cross section.

Figure 8 shows a concentration of strength near 50 keV. Only two of these resonances correspond to *s*-wave neutron transitions (arrows). Therefore, most of the resonances are probably  $\frac{3}{2}^+$  resonances which can be excited by *E1* photons from the ground state of  $^{57}\text{Fe}$  and which decay by *d*-wave neutrons. Since these neutron widths are too small to measure, no additional information for this possible  $\frac{3}{2}^+$  doorway state can be obtained from the neutron channel. However, if it could be shown from angular distribution measurements that most of the peaks in this region do actually have  $J = \frac{3}{2}$ , this would provide additional evidence for a doorway-state assignment. (Again, an *M1* doorway state with  $J^\pi = \frac{1}{2}^-$  or  $\frac{3}{2}^-$  is possible.) It should be noted that the peaks in this energy region have not been shown definitely to result from ground-state transitions.<sup>14,26</sup> Even so, if most of them decay to a common excited state of  $^{56}\text{Fe}$ , a doorway state still could be present, but at a higher excitation energy in  $^{57}\text{Fe}$ .

#### D. $^{57}\text{Fe}$ near 250 keV

Much of the  $^{57}\text{Fe}(\gamma, n)$  cross section in the ener-

gy region from 0 to 500 keV is made up of  $\frac{1}{2}^+$  *s*-wave resonances, as indicated by the arrows in Figs. 8 and 9. The values of  $\Gamma_{\gamma 0}$  for these  $\frac{1}{2}^+$  resonances are represented by the arrows shown in Fig. 10. These values of  $\Gamma_{\gamma 0}$  form an envelope centered near 250 keV, and appear to indicate the presence of a doorway state. However, no supporting evidence for the doorway is seen in the neutron channel. The reduced neutron widths<sup>5</sup> for these resonances do not show an envelope, and the rank correlation coefficient between the neutron and  $\gamma$ -ray widths is 0.20. This structure, then, either represents a  $\frac{1}{2}^+$  doorway state with  $\gamma$ -ray strength but very little neutron strength, or it is caused simply by statistical fluctuations in the  $\gamma$ -ray widths. The analysis of Sec. III indicates that intermediate structures containing 14 or more resonances are generated at the rate of 1 per 100 resonances, or, for the spacing of  $\frac{1}{2}^+$  resonances in  $^{57}\text{Fe}$ , 1 per 3600 keV.

#### VI. CHANNEL-RESONANCE EFFECT

The channel-resonance effect of Lane and Lynn<sup>18</sup> is another mechanism that can give rise to correlations between neutron and  $\gamma$ -ray widths. These authors, in formulating a model to explain a direct-capture mechanism in the  $(n, \gamma)$  reaction, predict three terms contributing to the cross section: (1) the ordinary resonance compound-nucleus term; (2) a resonant term from the channel (outside the nucleus) region; and (3) a nonresonant contribution from the channel region. The first

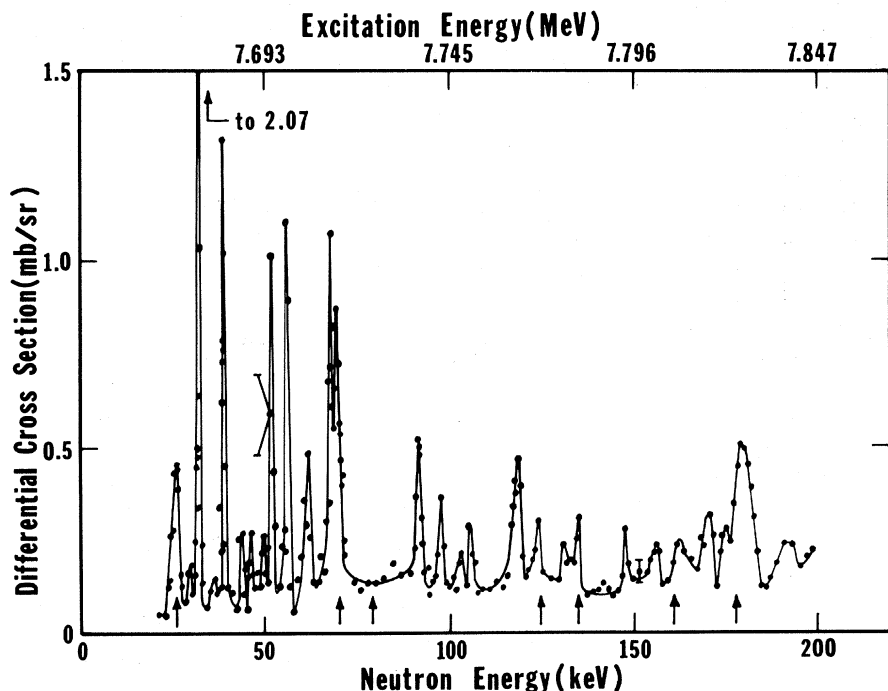


FIG. 8. The 135° differential  $^{57}\text{Fe}(\gamma, n)$  cross section from 0 to 200 keV. Arrows below the data indicate the positions of  $\frac{1}{2}^+$  states determined in the measurement of  $^{56}\text{Fe}(n, n)$  (Ref. 5).

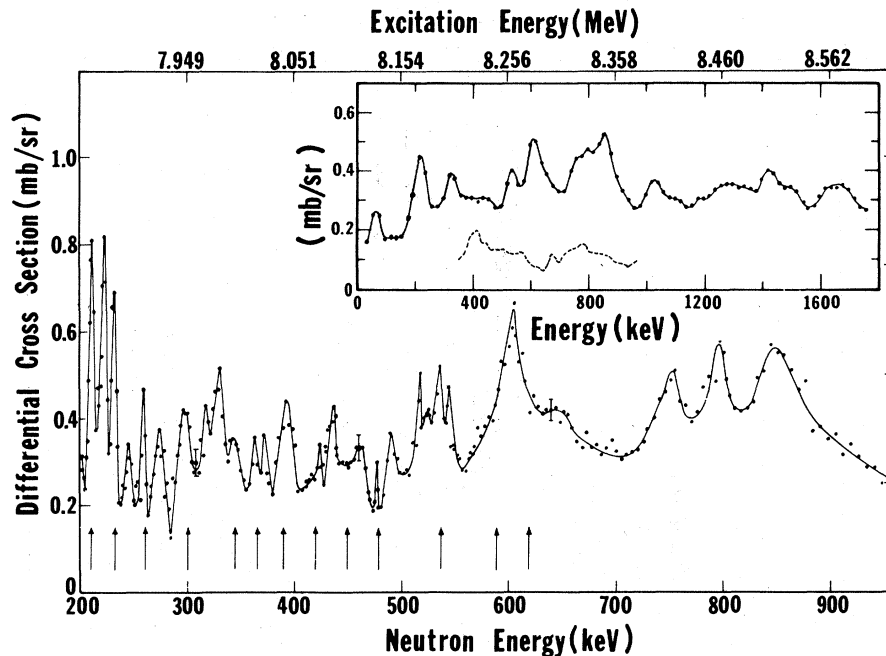


FIG. 9. The  $135^\circ$  differential  $^{57}\text{Fe}(\gamma, n)$  cross section from 200 to 950 keV. Arrows below the data indicate the positions of  $\frac{1}{2}^+$  states determined in the measurement of  $^{56}\text{Fe}(n, n)$  (Ref. 5). The inset shows the  $^{57}\text{Fe}(\gamma, n)$  cross section averaged with a 40-keV square smoothing function. The dashed curve in the inset is the averaged  $^{56}\text{Fe}(n, n)$  cross section from Ref. 25.

two terms have the same energy dependence (Breit-Wigner) and can be combined into one term whose  $\gamma$ -ray width can be written as:

$$\Gamma_{\gamma\lambda} = \Gamma_{\gamma\lambda}^{(1)} + \Gamma_{\gamma\lambda}^{(2)}, \quad (7)$$

where  $\Gamma_{\gamma\lambda}$  is the  $\gamma$ -ray width for transitions from a compound-nucleus state  $\lambda$  to a final state  $f$ , and  $\Gamma_{\gamma\lambda}^{(1)}$  and  $\Gamma_{\gamma\lambda}^{(2)}$  are the widths arising, respectively, from the first and second cross-section terms above. Lane and Lynn show that  $\Gamma_{\gamma\lambda}^{(2)}$  is proportion-

al to the reduced neutron width of the capturing state,  $\Gamma_{n\lambda}^0$ , and the single-particle width of the final state,  $S_f$ . Thus, Eq. (7) can be written as

$$\Gamma_{\gamma\lambda} = \Gamma_{\gamma\lambda}^{(1)} + K S_f \Gamma_{n\lambda}^0, \quad (8)$$

indicating a correlation between the neutron and  $\gamma$ -ray widths for the capturing states  $\lambda$ . Since the channel-resonance term has the same energy dependence as the compound-nucleus term, the only way of detecting the former is by observing a correlation. Lone *et al.*,<sup>27</sup> in the study of  $^{169}\text{Tm}(n, \gamma)$ , observed a correlation between neutron and  $\gamma$ -ray widths and interpreted this as evidence for the channel-resonance effect.

In this work we have attempted to find a correlation between the values for  $\Gamma_{\gamma\lambda}$  and those for  $\Gamma_{n\lambda}^0$  for  $s$ -wave states in  $^{57}\text{Fe}$  and  $^{53}\text{Cr}$ . In the case of  $^{57}\text{Fe}$ , 11  $\frac{1}{2}^+$  states were observed, between 25 and 320 keV, in the measurement<sup>5</sup> of the neutron total cross section of  $^{56}\text{Fe}$ . (The questionable states at 124 and 164 keV are neglected here.) 10 of these states were observed in the present  $^{57}\text{Fe}(\gamma, n)$  cross section and the 11th state was assigned  $\Gamma_{\gamma\lambda} = 0$ . Using Eq. (6), the correlation coefficient between the values for  $\Gamma_{\gamma\lambda}$  and those for  $\Gamma_{n\lambda}^0$  was calculated to be 0.14.

Figures 11 and 12 show the  $^{53}\text{Cr}(\gamma, n)$  cross section. This was measured<sup>14</sup> using the multiplicity

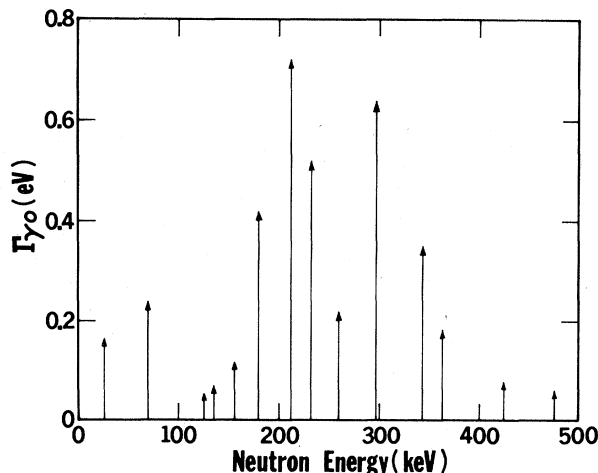


FIG. 10. Values for  $\Gamma_{\gamma 0}$  for  $\frac{1}{2}^+$  resonances in  $^{57}\text{Fe}$ .

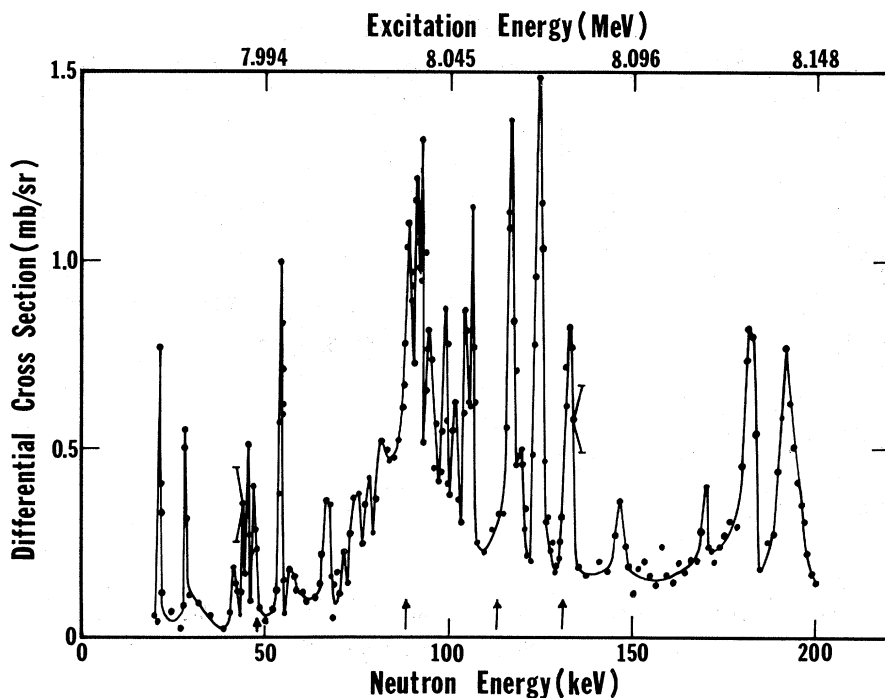


FIG. 11. The  $135^\circ$  differential  $^{53}\text{Cr}(\gamma, n)$  cross section from 0 to 200 keV. Arrows below the data indicate the positions of  $\frac{1}{2}^+$  states determined in the measurement of  $^{52}\text{Cr}(n, n)$  (Ref. 5).

detector with an end-point energy of 11.5 MeV. The sample was 52 g of  $\text{Cr}_2\text{O}_3$  enriched to 95.56% in  $^{53}\text{Cr}$ . The structure near 100 keV appears to represent a possible doorway state. However, Jackson<sup>26</sup> has shown that several of these states correspond to neutron transitions to excited states and that the remaining states all do not have the same  $J^\pi$ , thus ruling out a possible doorway-state assignment from the ground-state cross-section data alone.

The arrows below the data indicate the positions of  $\frac{1}{2}^+$  states as determined by neutron total cross-section measurements<sup>5</sup> on  $^{52}\text{Cr}$ . In that experiment, 12  $\frac{1}{2}^+$  states were observed between 40 and 530 keV. In this work, only eight of these peaks were observed. One of the peaks that was not seen, at 113 keV, has a narrow total width and would have been seen easily if it had sufficient  $\gamma$ -ray strength (area  $\propto g_\gamma \Gamma_{\gamma 0}$ ). Therefore,  $\Gamma_{\gamma\lambda} = 0$  is assigned for this peak. The other three remaining peaks with neutron energies of 93.5, 138.0, and 146.1 keV have large total widths. Therefore, these peaks might have sufficient  $\gamma$ -ray strength which, instead of being observed in the form of a resonance, is spread out and appears as background underlying narrow resonances. Hence, the value  $\Gamma_{\gamma\lambda}$  cannot be assigned for these peaks; instead they are ignored in the analysis. The correlation coefficient between the neutron and  $\gamma$ -ray

widths for the nine states considered is 0.07.

If the number of resonances incorporated into the statistical analysis is relatively small (less than 20, say), the resulting distribution of correlation coefficients is not sharply peaked around zero, and a value for the correlation coefficient less than about 0.2 easily can be generated from random effects alone. Therefore, for both  $^{57}\text{Fe}$  and  $^{53}\text{Cr}$ , the correlation coefficient is not significantly different from zero, indicating the channel-resonance terms are small compared with the compound-nucleus terms.

## VII. SUMMARY

The doorway state in  $^{207}\text{Pb}$  near 500 keV above the  $(\gamma, n)$  threshold, which was discovered in the measurement of the neutron total cross section of  $^{206}\text{Pb}$ , also is observed here through the  $^{207}\text{Pb}(\gamma, n)$  reaction. The evidence for this doorway state appears in the form of an envelope of  $\gamma$ -ray widths, as well as a correlation between the neutron and  $\gamma$ -ray widths for the fine-structure resonances of the doorway. This correlation was used to determine the ground-state  $\gamma$ -ray width of the doorway state to be  $\Gamma_{\gamma 0}^D = 36.5 \pm 3.5$  eV. Evidence for an additional doorway state in  $^{207}\text{Pb}$  near 125 keV was observed in the form of another envelope of  $\gamma$ -ray widths and a peak in the averaged  $^{207}\text{Pb}(\gamma, n)$

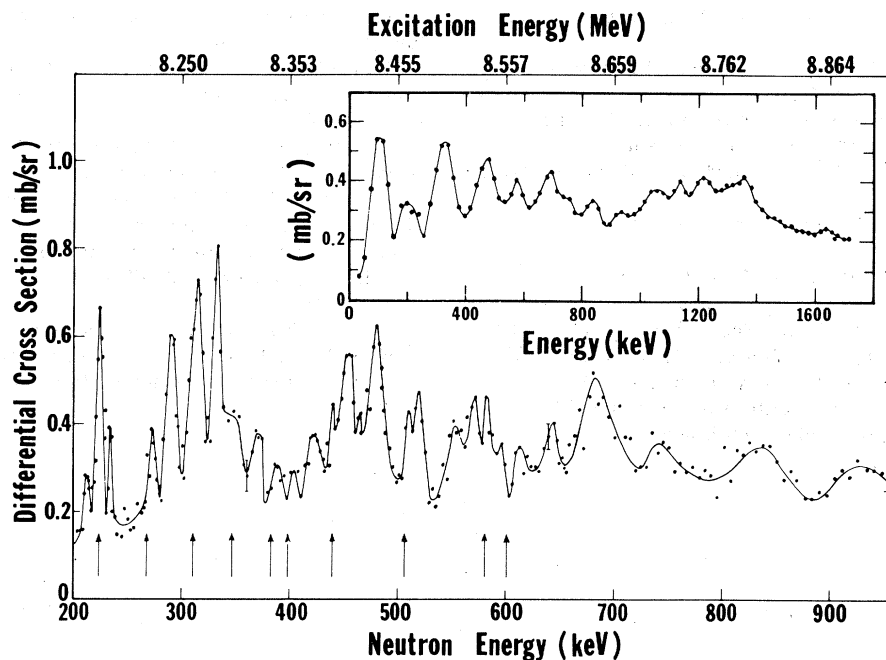


FIG. 12. The  $135^\circ$  differential  $^{53}\text{Cr}(\gamma, n)$  cross section from 200 to 950 keV. Arrows below the data indicate the positions of  $\frac{1}{2}^+$  states determined in the measurement of  $^{52}\text{Cr}(n, n)$  (Ref. 5). The inset shows the cross section averaged with a 40-keV square smoothing function.

cross section. This state probably has  $J^\pi = \frac{3}{2}^+$  and  $\Gamma_{\gamma 0}^D = 16.3$  eV.

Seven  $1^+$  states with a total  $\gamma$ -ray strength of 50.8 eV were observed in  $^{208}\text{Pb}(\gamma, n)$  near 500 keV. This concentration of  $M1$  strength can be explained on the basis of one-particle-one-hole excitations involving the  $i_{13/2}$  neutron and  $h_{11/2}$  proton shells. A concentration of strength near 50 keV in the  $^{57}\text{Fe}(\gamma, n)$  cross section might indicate the presence of a  $\frac{3}{2}^+$  doorway state. An envelope of values for  $\Gamma_{\gamma 0}$  for  $\frac{1}{2}^+$  levels near 250 keV in  $^{57}\text{Fe}(\gamma, n)$  was observed and might indicate the presence of a  $\frac{1}{2}^+$  doorway state. Finally, the correlation coefficient was calculated for the neutron and  $\gamma$ -ray widths for  $\frac{1}{2}^+$  states in  $^{57}\text{Fe}$  and  $^{53}\text{Cr}$  in an attempt to find

evidence for the channel-resonance effect of Lane and Lynn; no strong correlation was found.

#### ACKNOWLEDGMENTS

The authors are indebted to Dr. T. W. Phillips for assistance in some of the measurements, to Dr. A. K. Kerman, Dr. C. M. Shakin, and Dr. M. S. Weiss for several helpful conversations during the progress of this experiment, to Dr. H. W. Newson and Dr. J. A. Farrell for valuable discussions on the details of the neutron experiments, to Dr. E. G. Fuller for suggesting the use of the rank correlation coefficient, and to Dr. H. E. Jackson for communicating to us his results in advance of publication.

\*Work done under the auspices of the U. S. Atomic Energy Commission. Preliminary accounts of part of this work appeared as Bull. Am. Phys. Soc. **15**, 481, 85 (1970).

†Present address: Vanderbilt University, Nashville, Tennessee 37203.

<sup>1</sup>B. Block and H. Feshbach, Ann. Phys. (N.Y.) **23**, 47 (1963).

<sup>2</sup>H. Feshbach, A. K. Kerman, and R. H. Lemmer, Ann. Phys. (N.Y.) **41**, 230 (1967).

<sup>3</sup>J. P. Jeukenne and C. Mahaux, Nucl. Phys. **A136**, 49 (1969).

<sup>4</sup>J. A. Farrell, G. C. Kyker, Jr., E. G. Bilpuch, and H. W. Newson, Phys. Letters **17**, 286 (1965).

<sup>5</sup>C. D. Bowman, E. G. Bilpuch, and H. W. Newson, Ann. Phys. (N.Y.) **17**, 319 (1962).

<sup>6</sup>C. Shakin, Ann. Phys. (N.Y.) **22**, 373 (1963).

<sup>7</sup>P. P. Singh, P. Hoffman-Pinther, and D. W. Lang, Phys. Letters **23**, 255 (1966).

<sup>8</sup>C. E. Porter and R. G. Thomas, Phys. Rev. **104**, 483 (1956).

<sup>9</sup>N. Rosenzweig, Phys. Rev. Letters **1**, 24 (1958).

<sup>10</sup>B. L. Berman, G. S. Sidhu, and C. D. Bowman, Phys. Rev. Letters **17**, 761 (1966).

- <sup>11</sup>C. D. Bowman, G. S. Sidhu, and B. L. Berman, *Phys. Rev.* **163**, 951 (1967).
- <sup>12</sup>C. D. Bowman, B. L. Berman, and H. E. Jackson, *Phys. Rev.* **178**, 1827 (1969).
- <sup>13</sup>R. J. Baglan, University of California Radiation Laboratory Report No. UCRL-50902 (unpublished).
- <sup>14</sup>R. J. Baglan, C. D. Bowman, and B. L. Berman, *Phys. Rev. C* **3**, 672 (1971).
- <sup>15</sup>H. Hotelling and M. Pabst, *Ann. Math. Stat.* **7**, 29 (1936).
- <sup>16</sup>E. G. Olds, *Ann. Math. Stat.* **9**, 133 (1938).
- <sup>17</sup>G. E. Brown, *Nucl. Phys.* **57**, 339 (1964).
- <sup>18</sup>A. M. Lane and J. E. Lynn, *Nucl. Phys.* **17**, 563 (1960).
- <sup>19</sup>R. L. Van Hemert, C. D. Bowman, R. J. Baglan, and B. L. Berman, *Nucl. Instr. Methods* **89**, 263 (1970); R. L. Van Hemert, University of California Radiation Laboratory Report No. UCRL-50501 (unpublished).
- <sup>20</sup>R. L. Macklin, P. J. Pasma, and J. H. Gibbons, *Phys. Rev.* **136**, B695 (1964).
- <sup>21</sup>E. G. Bilpuch, K. K. Seth, C. D. Bowman, R. H. Ta-bony, R. C. Smith, and H. N. Newson, *Ann. Phys. (N.Y.)* **14**, 387 (1961).
- <sup>22</sup>J. A. Biggerstaff, J. R. Bird, J. H. Gibbons, and W. M. Good, *Phys. Rev.* **154**, 1136 (1967).
- <sup>23</sup>C. D. Bowman, R. J. Baglan, B. L. Berman, and T. W. Phillips, *Phys. Rev. Letters* **25**, 1302 (1970).
- <sup>24</sup>M. S. Weiss, private communication.
- <sup>25</sup>J. E. Monahan and A. J. Elwyn, *Phys. Rev. Letters* **20**, 1119 (1968).
- <sup>26</sup>H. E. Jackson, private communication.
- <sup>27</sup>M. A. Lone, R. E. Chrien, O. A. Wasson, M. Beer, M. R. Bhat, and H. R. Muether, *Phys. Rev.* **174**, 1512 (1968).